Entanglement and quantum phase transition in the asymmetric Hubbard chain: density-matrix renormalization group calculations

2008 J. Phys.: Condens. Matter 20 345217

(http://iopscience.iop.org/0953-8984/20/34/345217)

IOP PUBLISHING JOURNAL OF PHYSICS: CONDENSED MATTER

J. Phys.: Condens. Matter **20** (2008) 345217 (8pp) doi:10.1088/0953-8984/20/34/345217

Entanglement and quantum phase transition in the asymmetric Hubbard chain: density-matrix renormalization group calculations

Wen-Ling Chan and Shi-Jian Gu[1]

Department of Physics and Institute of Theoretical Physics, The Chinese University of Hong Kong, Hong Kong, People's Republic of China

E-mail: sjgu@phy.cuhk.edu.hk

Received 15 May 2008, in final form 14 July 2008
Published 1 August 2008
Online at stacks.iop.org/JPhysCM/20/345217

Abstract

We study the ground state quantum phase transition by means of entanglement in the one-dimensional asymmetric Hubbard model with open boundary conditions. The local entanglement between the middle two sites and the rest of the system, and the block entanglement between the left and right portions of the system, are calculated using the density-matrix renormalization group (DMRG) method. We find that the entanglement shows interesting scaling and singular behavior around the phase transition line.

(Some figures in this article are in colour only in the electronic version)

1. Introduction

In condensed-matter physics, given a quantum system, some of the most challenging problems are to find the ground state and to study the quantum phase transition [1]. For those models without analytical solutions the general approach is to characterize an order parameter and measure it from the ground state obtained numerically from a finite system, then do scaling studies and extrapolate the results to the thermodynamic limit. However, in some cases this method is quite inefficient and sometimes no definite conclusion can be drawn.

Recently it had been shown that entanglement [2] may be an effective indicator of quantum phase transition in spin systems [3–5]. This concept was also applied to fermionic systems [6] including the extended Hubbard model [7–9], ionic Hubbard model [10], asymmetric Hubbard model [11] and some other related models [12]. Gu *et al* [8] studied the extended Hubbard model and found that the local entropy, that is the entanglement between one site and the rest of the system, clearly indicates that phase transition occurs where the entropy is extremum or its derivative is singular. Legeza *et al* [10] showed that in some models the two-site entropy is a better indicator. These entropies can be readily obtained using the density-matrix renormalization group (DMRG) method [13, 14].

In this paper we use entanglement to demonstrate the phase transition of the one-dimensional asymmetric Hubbard model (AHM) with open boundary conditions. In the AHM there are two species of fermions, say spin ↑ and spin ↓ particles, with different masses. The model has been intensively studied recently as it may be used to describe some important physical properties in strongly correlated systems such as superconducting cuprates [15] and heavy fermionic systems [16]. It can be realized in experiments using cold fermionic atoms trapped in optical lattices [11, 17, 18], where all model parameters can be tuned. It has also been studied theoretically [11, 19–22]. However, the complete phase diagram is still not very clear.

We consider equal number of both species of fermions. We numerically calculate the two-site entropy as well as the block entropy [4], which is defined as the entanglement between the left and right portions of the system. We propose that the entanglement shows interesting scaling behavior around the phase transition line.

[1] http://www.phystar.net

The Hamiltonian of the AHM reads

$$H = -\sum_{\langle ij\rangle}\sum_{\sigma=\uparrow,\downarrow} t_\sigma c^\dagger_{i\sigma} c_{j\sigma} + U\sum_i n_{i\uparrow} n_{i\downarrow}, \tag{1}$$

where $t_\uparrow \geqslant t_\downarrow \geqslant 0$ are the hopping integrals for the light $\uparrow$ and heavy $\downarrow$ fermions, respectively, $c^\dagger_{i\sigma}$ and $c_{i\sigma}$ are the creation and annihilation operator, respectively, $U > 0$ is the on-site repulsive Coulomb interaction between the two species of fermions, and $n_{i\sigma} = c^\dagger_{i\sigma} c_{i\sigma}$ is the number operator. Hereafter we set $t_\uparrow = 1$. The AHM reduces to the Hubbard model (HM) [23–25] for $t_\uparrow = t_\downarrow = 1$ and to the Falicov–Kimball model (FKM) [26–30] for $t_\downarrow = 0$. We only consider the cases with $N_\uparrow = N_\downarrow$. The filling density is defined as $n = (N_\uparrow + N_\downarrow)/L$, where L is the length of the chain, or the number of sites. Half-filling ($n = 1$) is achieved when $N_\uparrow = N_\downarrow = L/2$.

It is well known that the HM and FKM belong to different universality classes [19]. A phase transition should occur somewhere on the U–$t_\downarrow$ plane [18–20]. To understand the phases, we first look at the perturbation expansion in the large-U limit. When $t_\uparrow, t_\downarrow \ll U$, the hopping term in Hamiltonian (1) can be regarded as a small perturbation. For the HM, provided that $n \leqslant 1$, the expansion leads effectively to the t–J model [31]. The method can be generalized to the AHM [19]. Since the calculation is straightforward but lengthy, we only present the final result. The expansion leads effectively to the anisotropic Heisenberg model with hopping. Explicitly the effective Hamiltonian reads

$$\begin{aligned} H_{\text{eff}} = &-\sum_{\langle ij\rangle}\sum_{\sigma=\uparrow,\downarrow} t_\sigma \tilde{c}^\dagger_{i\sigma}\tilde{c}_{j\sigma} \\ &+ \frac{t_\uparrow t_\downarrow}{U}\sum_{\langle ij\rangle}[\sigma^x_i\sigma^x_j + \sigma^y_i\sigma^y_j + \Delta(\sigma^z_i\sigma^z_j - 1)] \\ &+ \mathrm{O}\left(\frac{t^4_\sigma}{U^3}\right), \end{aligned} \tag{2}$$

in which

$$\tilde{c}^\dagger_{i\sigma} = (1 - n_{i\bar{\sigma}})c^\dagger_{i\sigma}, \tag{3}$$

$$\Delta = \frac{t^2_\uparrow + t^2_\downarrow}{2t_\uparrow t_\downarrow} \geqslant 1, \tag{4}$$

where $\bar{\sigma}$ denotes the opposite spin of σ.

At $n = 1$, $\tilde{c}^\dagger_{i\sigma}$ and $\tilde{c}_{j\sigma}$ can be approximated as zero in the large-U limit, hence the hopping term in the effective Hamiltonian vanishes and the effective model becomes the anisotropic Heisenberg model (the XXZ model). Therefore, the system behaves very differently at $n = 1$ and $n < 1$. The case $n > 1$ can be treated by considering the particle–hole symmetry [32] of the AHM. It is found that the energy spectrum is invariant (except for a global shift by a constant) under the exchange of the numbers of particles and holes, hence the physical properties of the system at $n > 1$ are just the same as that at $n < 1$.

Away from half-filling (either $n < 1$ or $n > 1$), the system possesses the density wave (DW) phase and phase separation (PS) phase [28, 33]; at half-filling ($n = 1$), the system possesses effectively the XY phase and the Ising phase.

The paper is arranged as follows. In section 2 we show how entanglement is measured and implemented in the DMRG algorithm. In section 3 we give the numerical results and discussions for the away-from-half-filling and half-filling cases, respectively. Finally a summary is given in section 4.

2. Measurement of entanglement

We are interested in the entanglement between a local block, which is composed of one or more sites, and the rest of the system. For the AHM, the local state on each site has four possible configurations: $|0\rangle$, $|\uparrow\rangle$, $|\downarrow\rangle$ and $|\uparrow\downarrow\rangle$. The Hilbert space associated with the system with L sites is spanned by 4^L basis vectors. Suppose we have obtained the ground state $|\Psi\rangle$, the reduced density matrix of the local block with l sites is

$$\rho_l = \mathrm{tr}_{L-l}|\Psi\rangle\langle\Psi|. \tag{5}$$

This matrix can be expressed in block diagonal form due to the fact that the numbers of $\uparrow$ and $\downarrow$ fermions are conserved:

$$\rho_l = \mathrm{diag}\{(0,0),(1,0),(0,1),(1,1),\ldots,(l,l)\}, \tag{6}$$

where (m, n) means a block whose bases contain m $\uparrow$ and n $\downarrow$ fermions. The von Neumann entropy

$$S_l = -\mathrm{tr}\left[\rho_l \log_2(\rho_l)\right] \tag{7}$$

measures the entanglement between the l sites and the remaining $L-l$ sites of the system. In general, the more evenly distributed the eigenvalues of ρ_l, the higher the entropy is. The degree of freedom (and hence the number of bases) within a block of length l is 4^l, therefore there are 4^l eigenvalues. The entropy S_l is maximum when all eigenvalues are equal ($= 4^{-l}$), and so $S_{l,\max} = -\log_2 4^{-l} = 2l$.

We use the DMRG method [13, 14] to calculate the ground state properties of the system. This method is efficient and accurate for one-dimensional lattice models. It involves iterative diagonalization of a Hamiltonian in an approximated, size-limited Hilbert space to obtain the target state (usually the ground state). The approximated Hilbert space is constructed from an appropriate number of eigenvectors of the reduced density matrix of part of the system.

We are interested in two quantities: the two-site entropy and the block entropy. Conceptually they are the same kind of measurement. Both of them are the von Neumann entropy of the reduced density matrix of part of the chain. The two-site entropy, denoted as S_2, is defined as the entanglement between the middle two consecutive sites with the rest of the system. We choose the middle sites so as to minimize any boundary effects. Note that we consider the chain with an even number of sites only. The measurement can be easily implemented in the DMRG method [10]. During a 'sweep' in the finite lattice algorithm, when the two free sites 'move' to the middle, we obtain their reduced density matrix and compute the von Neumann entropy using equation (7).

On the other hand, the block entropy, denoted as $S(l)$, is defined as the entanglement between the left block consisting of l sites and the remaining right block. Studies of this quantity have established a bridge between the quantum information theory and conformal field theory [4, 34, 35]. In the DMRG

algorithm the left and right blocks are renormalized in each step. The well-known fact that the entropy does not change upon renormalization group transformation enables us to obtain the required block entropy.

In the DMRG method we apply the dynamical block selection approach [36] plus information loss control [37] to increase the efficiency and accuracy. In the following computations we set the information loss $\chi < 10^{-8}$ and the minimum and maximum number of DMRG states to be 100 and 250, respectively. Also, we apply the seed vector construction routine [38] to further improve the efficiency.

3. Numerical results

3.1. Away from half-filling

In this section we examine the system where the total number of particles does not equal L. In particular, we study 1/4-filling, that is $N_\uparrow = N_\downarrow = L/4$ and $n = 1/2$. Before presenting the results of the entanglement measurements, we would first like to clarify the phases.

When $t_\uparrow$ is much larger than $t_\downarrow$ in magnitude, the hopping of the light $\uparrow$ fermions becomes much more helpful for lowering the system's energy than that of the heavy $\downarrow$ fermions. The appropriate configuration is that the light fermions spread around in a large pool of free sites while the heavy fermions congregate together. The two species of fermions separate, hence the name phase separation (PS) phase to describe the system. For open boundary conditions, as in our case, the light fermions tend not to stay at the ends of the chain as it is too costly to sacrifice some freedom of hopping, hence it is the heavy ones which fill the ends. The following shows a typical dominant configuration in this phase (24 sites, 1/4-filling):

$$|\downarrow\downarrow\downarrow 0 \uparrow 00 \uparrow 0 \uparrow 00 \uparrow 00 \uparrow 00 \uparrow 00 \downarrow\downarrow\downarrow\rangle. \qquad (8)$$

On the other hand, when $t_\uparrow \approx t_\downarrow$, the hopping of each species of fermion is equally important. It turns out that both of them distribute uniformly on the whole chain and the system is in the so-called density wave (DW) phase. A typical dominant configuration is

$$|\downarrow 0 \uparrow 0 \downarrow\uparrow 0 \downarrow 00 \uparrow 0 \downarrow 0 \uparrow 0 \downarrow 00 \uparrow\downarrow 0 \uparrow 0\rangle. \qquad (9)$$

Our conjecture can be verified by measuring the local densities of the $\uparrow$ and $\downarrow$ fermions. Figure 1 shows the results for a chain of 16 sites with 4 $\uparrow$ and 4 $\downarrow$ fermions. Clearly, for small $t_\downarrow$, the density of the heavy $\downarrow$ fermions is much higher at the two ends of the chain (PS phase), while for large $t_\downarrow$, the density distribution is more even (DW phase).

Then we compute the two-site entropy S_2 for different values of $t_\downarrow$ and U using the DMRG method. Figures 2(a) and (b) show the results for $U = 6.0$ and 20.0, respectively. It is obvious that, for any given L, two plateaus appear. For small $t_\downarrow$ (PS phase) S_2 is lower, while for large $t_\downarrow$ it is higher. The cliff connecting the two plateaus becomes steeper and steeper as L increases. This property is clearly revealed when we plot the first derivatives of the curves in the insets. For any fixed L, a peak appears between the two phases. The peak

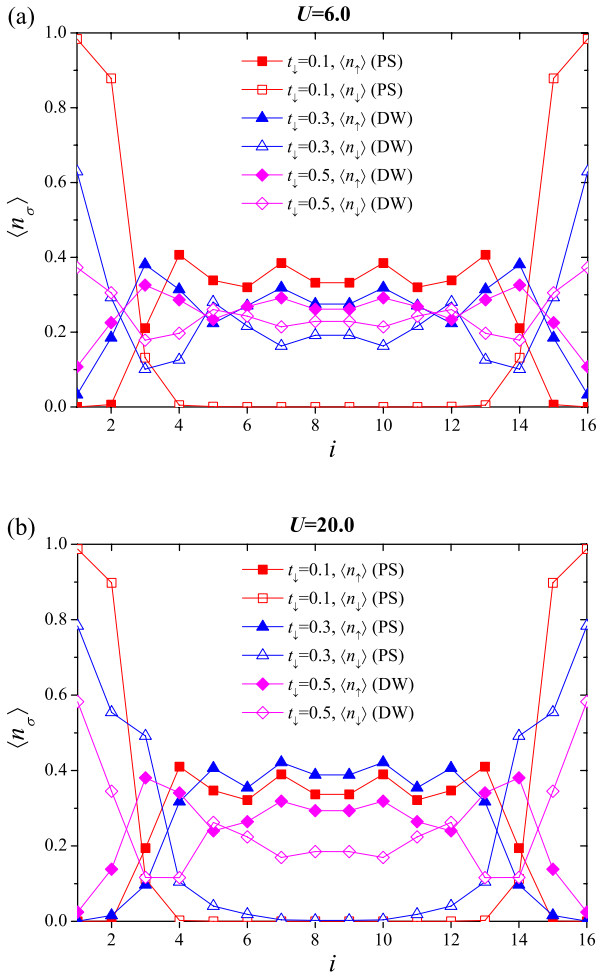

Figure 1. The number densities of $\uparrow$ and $\downarrow$ fermions at site i for a chain of length $L = 16$ at 1/4-filling: (a) $U = 6.0$, (b) $U = 20.0$.

is sharper for a longer chain. It may be expected that in the thermodynamic limit the peak goes to infinity, indicating that this phase transition is a typical Landau one.

Comparing the $U = 6.0$ and 20.0 cases, the critical $t_\downarrow$ is larger for larger U. This result is consistent with reference [11]. For the case $U = 6.0$, all curves seem to pass through the same point at $t_\downarrow = 0.170$. However, we check that this does not happen for other values of U. For instance, for $U = 1.0$ (which is not shown here), some curves do not even cross in the critical regime. Therefore the special crossing in the case $U = 6.0$ should merely be a coincidence.

It is not difficult to understand the phenomenon that the two-site entropy of the PS phase is lower than that of the DW phase. According to equation (6), the two-site reduced density matrix ρ_2 consists of nine blocks. In the PS phase, the heavy $\downarrow$ fermions congregate at the two ends while the light $\uparrow$ fermions distribute in the middle. Only blocks (0, 0), (1, 0) and (2, 0) contain significant values, hence S_2 is low. However, in the DW phase, the blocks (0, 0), (1, 0), (0, 1) and (1, 1) contain significant values and so S_2 is higher.

The above study shows that the two-site entropy S_2 is a good indicator of phase transition. From the insets of figure 2, it is obvious that at a given U the critical $t_\downarrow$ converges

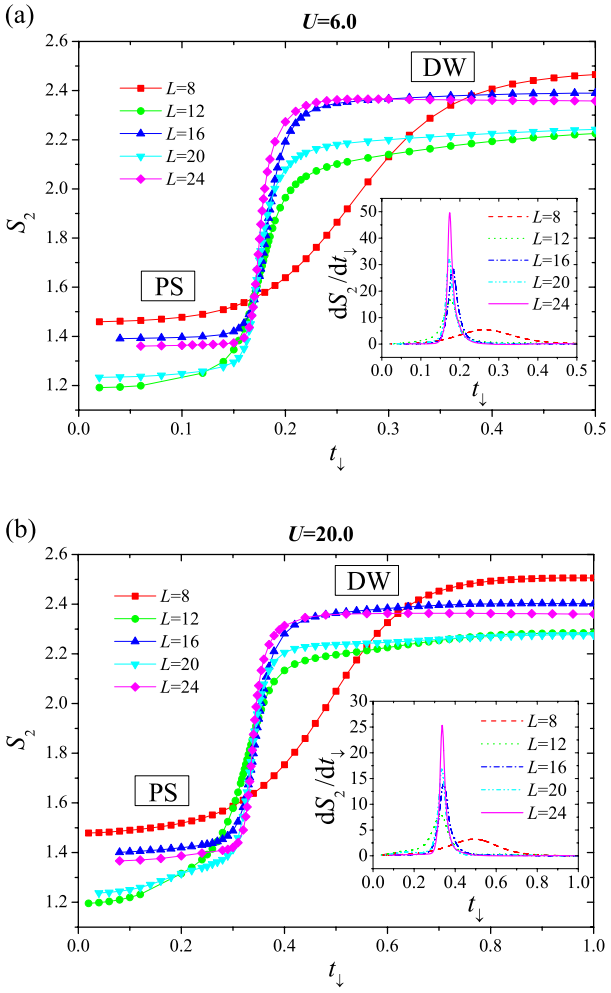

Figure 2. The two-site entropy S_2 against $t_\downarrow$ for different chain lengths L at 1/4-filling: (a) $U = 6.0$, (b) $U = 20.0$. The first derivatives are shown in the insets.

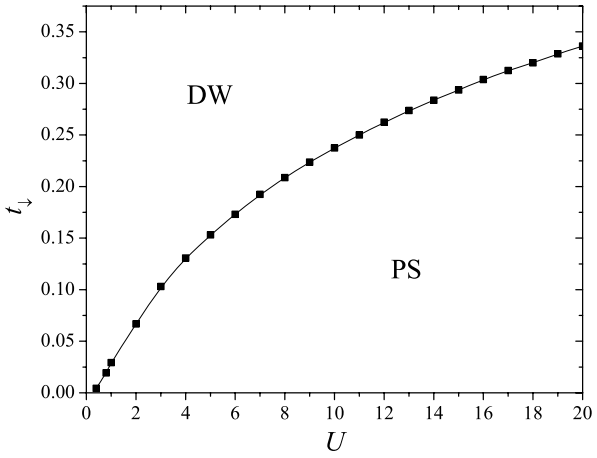

Figure 3. Ground state phase diagram of AHM at 1/4-filling in the thermodynamic limit, deduced by the singular behavior of the two-site entropy. The error bars are smaller than the size of the symbols.

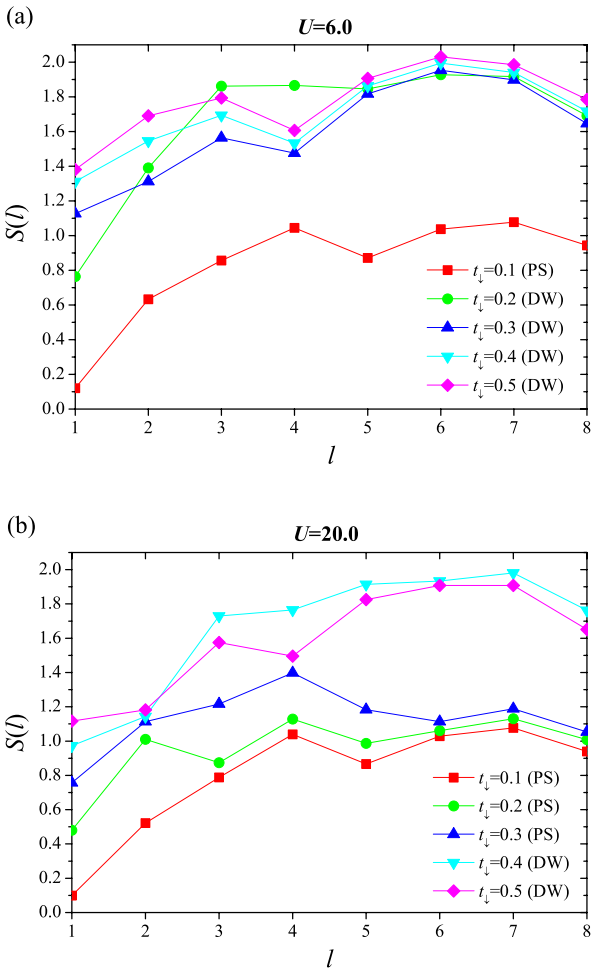

Figure 4. The block entropy $S(l)$ for different $t_\downarrow$ at 1/4-filling in a 16-site chain: (a) $U = 6.0$, (b) $U = 20.0$.

when L increases. The results can be extrapolated to the thermodynamic limit. We repeat the same analysis for different U and the phase transition line in the U–$t_\downarrow$ plane can be obtained, as presented in figure 3 with error bars smaller than the size of the symbols.

Next, we examine the block entropy of the same system. Figure 4 shows the results for a 16-site chain. Due to the symmetry $S(l) = S(L - l)$, it is sufficient to show $S(l)$ for $l = 1, \ldots, L/2$. First we note that in general $S(l)$ increases with l. This is not surprising because when the block becomes longer, there are more finite elements in the reduced density matrix ρ_l and hence higher $S(l)$. On the other hand, the block entropy in the DW phase is always higher than that in the PS phase. It is because, in the PS phase, only the matrix elements (in ρ_l) related to the bases where the $\downarrow$ fermions congregate to the left are significant; however, in the DW phase, many more elements are significant.

For small l, $S(l)$ fluctuates due to boundary effects, whereas it becomes more stable for long l. Moreover, the results show that $S(l)$ for different $t_\downarrow$ converge for long l. This indicates that the entropy of a longer block is a better indicator of phase transition. This conclusion is consistent with that in [10]. It is not surprising as the block entropy of a longer block includes more correlation functions. It is a pity that the convergence in the DMRG algorithm is poor for the AHM

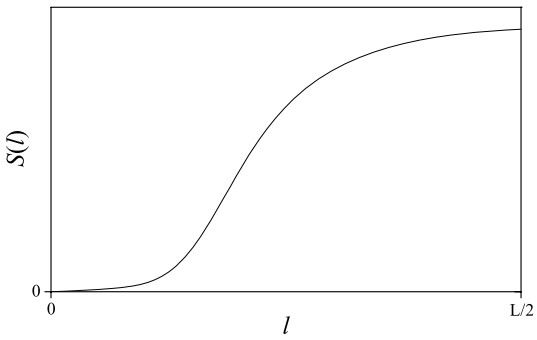

Figure 5. Proposed schematic sketch of the block entropy $S(l)$ against block length l at the ground state in the PS phase of a very long chain away from half-filling.

away from half-filling. The poor convergence is largely due to the fact that approximations to the particle densities have been unavoidably imposed during the infinite lattice algorithm (this problem does not exist for the half-filling case). Results obtained from longer chains are not quite reliable.

For a very long chain we suggest that $S(l)$ should behave as schematically sketched in figure 5. The rise of $S(l)$ is suppressed at the beginning as there is only one significant configuration (in which all sites contain the $\downarrow$ fermions) and hence $S(l)$ is close to zero. As the block grows and reaches the pool of $\uparrow$ fermions, $S(l)$ rises rapidly. For long l, the increase in the number of possible configurations is restricted due to the fact that the number of $\uparrow$ fermions is limited, hence $S(l)$ rises more slowly and soon saturates.

3.2. Half-filling

The physics of AHM at half-filling is quite different from that away from half-filling. In the large-U limit, the system at half-filling possesses two phases: the Hubbard phase (effectively the XY phase) for large $t_\downarrow$ and the FK phase (effectively the Ising phase) for small $t_\downarrow$. The transition is known to be Kosterlitz–Thouless like [39, 40]. The ground state phase diagram on the U–$t_\downarrow$ plane, unlike that in the previous case of away from half-filling, is more subtle and hard to complete. Fáth *et al* [19] studied the perturbation expansion and found that in the large-U limit the phase transition line is right on the Hubbard line $t_\downarrow = 1$. For small U they computed the spin gap and the magnetic order parameter; however, no solid conclusion could be drawn. In this section we make an attempt using entanglement.

First we compute the two-site entropy against $t_\downarrow$ for different L. The results are shown in figure 6. There are roughly two regions. For small $t_\downarrow$, S_2 presents algebraic scaling with $t_\downarrow$ (FK phase), while for large $t_\downarrow$, S_2 scales linearly with $t_\downarrow$ (Hubbard phase). The curves do not show discontinuity for higher derivatives even for long L. This is a property of the Kosterlitz–Thouless like transitions [39, 40], as explained in [6].

The finite-size effects give rise to the formation of two families of curves. One family is $L = 4m$ ($m = 1, 2, \ldots$) which has higher S_2, while the other one is $L = 4m + 2$ which has lower S_2. The explanation is as follows. On the chain,

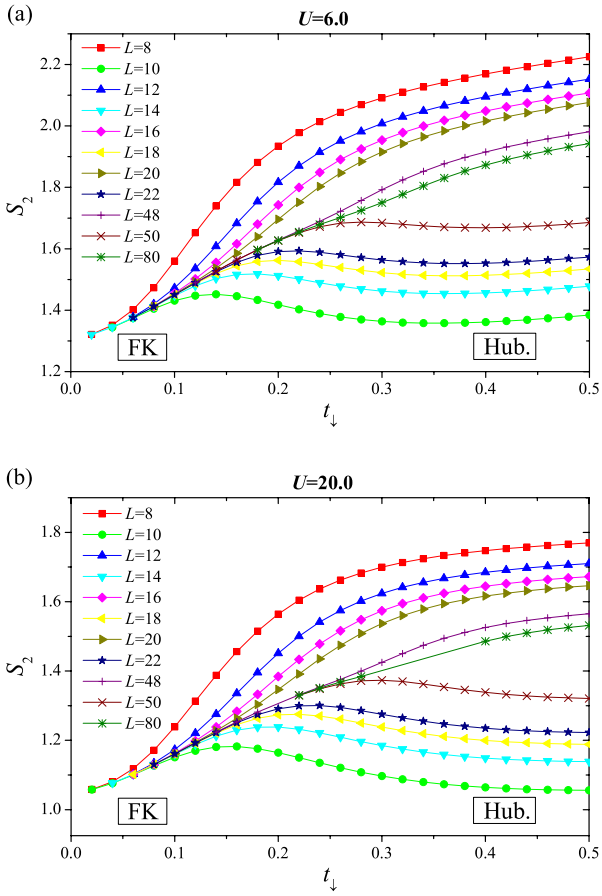

Figure 6. The two-site entropy S_2 against $t_\downarrow$ for different chain lengths L at half-filling: (a) $U = 6.0$, (b) $U = 20.0$.

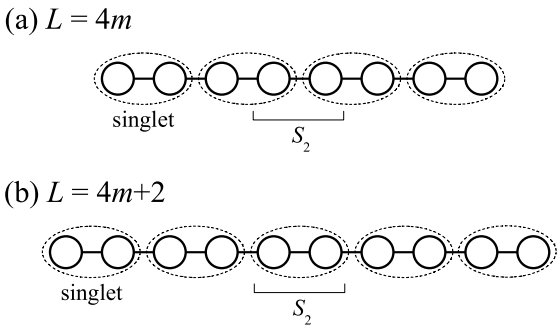

Figure 7. Schematic diagrams showing the configurations of singlets. (a) For the family $L = 4m$ (here $L = 8$), the middle two sites are little correlated, hence the entropy S_2 is higher. (b) For the family $L = 4m + 2$ (here $L = 10$), the middle two sites are strongly correlated, hence S_2 is lower.

the first site tends to form a singlet $(|\uparrow\downarrow\rangle - |\downarrow\uparrow\rangle)/\sqrt{2}$ with the second site so as to lower the energy of the system. The third site tends to form a singlet with the fourth one, and so on. Figure 7 schematically presents this phenomenon. If $L = 4m$, the middle two sites are from different singlets and hence little correlated. The spin freedom is higher, the uncertainty is more and therefore the entropy S_2 is higher. On the other hand, if $L = 4m + 2$, the middle two sites tend to form a singlet and

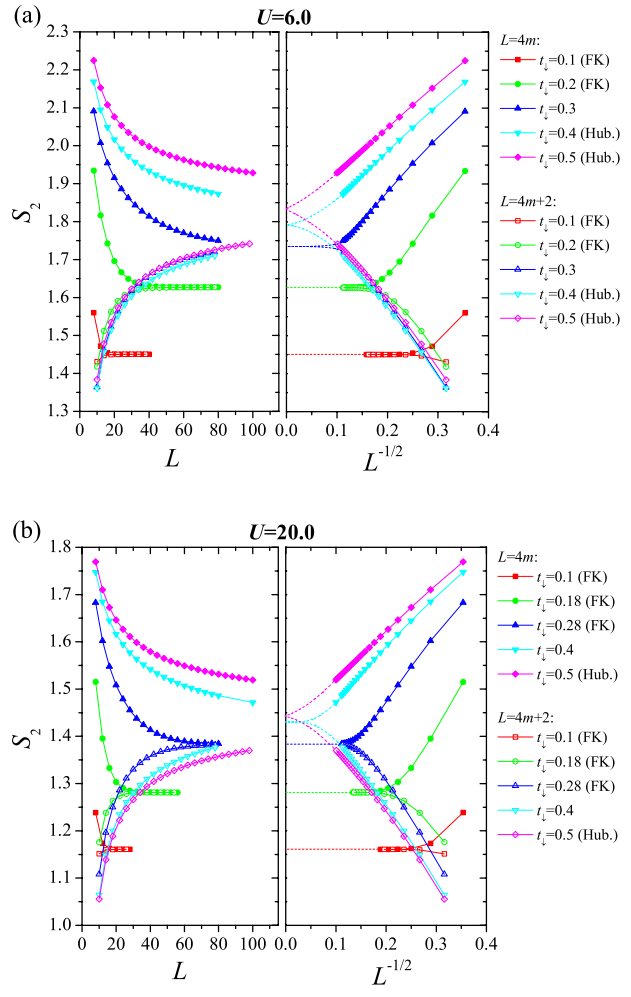

Figure 8. The two-site entropy S_2 versus chain length L or $1/\sqrt{L}$ for different $t_\downarrow$ at half-filling: (a) $U = 6.0$, (b) $U = 20.0$. Determinations of phase are suggested in the brackets.

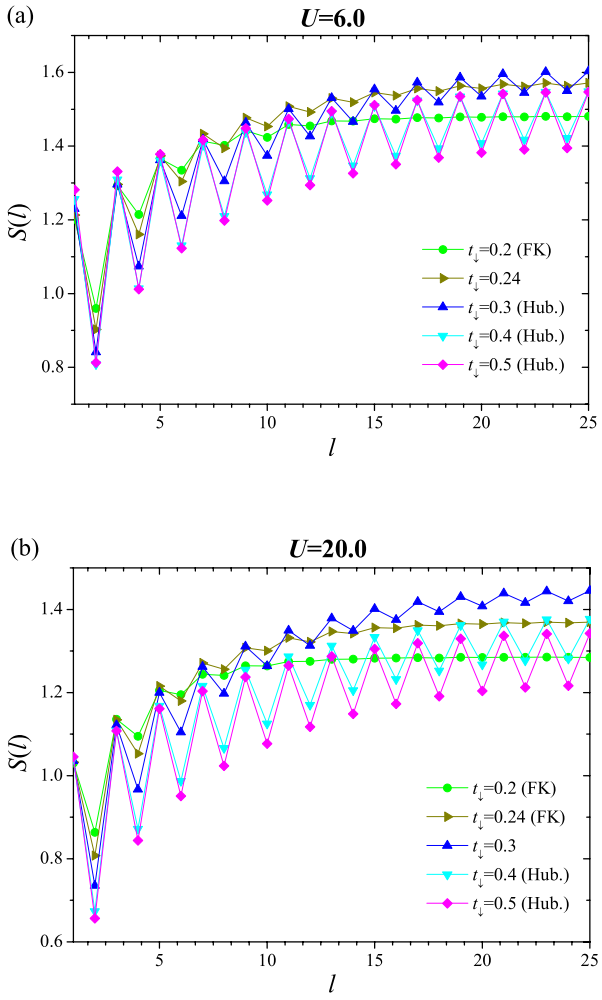

Figure 9. The block entropy $S(l)$ for different $t_\downarrow$ in a half-filling 50-site chain: (a) $U = 6.0$, (b) $U = 20.0$. Determinations of phase are suggested in the brackets.

hence are strongly correlated. The spin freedom is lower, the uncertainty is less and therefore S_2 is lower. We have verified this by measuring two-site entropies on different parts of the chain. When L increases, the two families tend to merge together. It is expected that in the thermodynamic limit they should no longer be distinct since all finite-size effects vanish.

Besides, the curves converge to a single point for $t_\downarrow \to 0$. In the $U \to \infty$ limit, the point is expected to be at $S_2 = 1.0$. This can be explained as follows. In the limits $U \to \infty$ and $t_\downarrow \to 0$, the effective Hamiltonian reduces to the Ising model. The ground state is doubly degenerate and the two configurations are $|\uparrow\downarrow\uparrow\downarrow\cdots\uparrow\downarrow\rangle$ and $|\downarrow\uparrow\downarrow\uparrow\cdots\downarrow\uparrow\rangle$. For a finite system the ground state is the symmetric combination of the two, hence $S_2 = 1.0$ for any even L.

The two-site entropy also presents different scaling behavior with L in the two phases. Figure 8 presents S_2 versus L and $1/\sqrt{L}$. The two families of curves ($L = 4m$ and $L = 4m + 2$) are indicated with distinct lines. From the shape of the lines we suggest which phase each line belongs to. Some lines belong to the critical regime between the two phases. In the FK phase, S_2 goes like $A(L \to \infty) + B\exp(-L/\xi)$ where A, B and ξ are parameters that may depend on $t_\downarrow$, U and L. B is positive for $L = 4m$ and negative for $L = 4m + 2$. For smaller $t_\downarrow$, S_2 converges more quickly. The physical interpretation is that the state is more ordered. In the Hubbard phase, S_2 goes like $C(L \to \infty) + D/\sqrt{L}$, where C and D may also depend on $t_\downarrow$, U and L. D is positive(negative) for $L = 4m$ ($L = 4m + 2$).

We expect the two families of curves for a certain $t_\downarrow$ to converge to the same value of S_2 in the thermodynamic limit, as the value should be independent of the parity and boundary condition of the chain. In the figures we extrapolate the curves and deduce the value in the limit.

Second, we compute the block entropy. Figure 9 shows the results for a 50-site chain. Again, due to the reflection symmetry $S(l) = S(L - l)$, it is sufficient to show $S(l)$ for $l = 1, \ldots, L/2$. In general $S(l)$ increases with l, for the same reason given in the previous section for the case of away from half-filling: when the block grows, the size of the reduced density matrix ρ_l increases and the number of finite elements in it increases, so $S(l)$ rises. On the other hand, the block entropy fluctuates with respect to the parity of l. For even l, the block is composed of a neatly arranged series of two-site singlets and

hence $S(l)$ is lower. The fluctuation becomes weaker for long l as the inner sites have a reduced tendency to form singlets.

From the trend of the lines we suggest to which phase each line belongs. Some lines belong to the critical regime between the two phases. The behavior of $S(l)$ is obviously different in the two phases. In the Hubbard phase, for either parity of l, $S(l)$ rises algebraically, whereas in the FK phase, for either parity of l, $S(l)$ rises quickly and saturates because the state is more ordered. In the $U \to \infty$ and $t_\downarrow \to 0$ limits it should be expected that in the FK phase $S(l) \to 1.0$ for all l because the ground state is the symmetric combination of the two definite Ising configurations: $|\uparrow\downarrow\uparrow\downarrow\cdots\rangle$ and $|\downarrow\uparrow\downarrow\uparrow\cdots\rangle$.

Vidal *et al* [4] suggested that, due to conformal field theory,

$$S(l) \approx P + Q \ln l \tag{10}$$

for long l, where P and Q are parameters that may depend on $t_\downarrow$, U and L. In the 'non-critical regime' (FK phase here) $Q \approx 0$, while in the 'critical regime' (Hubbard phase here) Q is proportional to the 'central charge' of the conformal field theory and is finite. Therefore, the parameter Q can be regarded as an indicator for the phase transition. For finite systems where boundary effects are noticeable, equation (10) is valid only for l in the vicinity of $L/4$. Hence, we take Q as the value of the slope of the $S(l)$–$\ln l$ graph at $l \approx L/4$. Only the data points at odd l are used so that the fluctuation of the graph due to the open boundary effect does not affect our result. We pick three data points to measure the slope. Thus, Q is computed as the weighted average of the slope between the first and second point and the slope of the second and third point. Explicitly,

$$\begin{aligned} l_0 &= [L/4], \\ l_\pm &= l_0 \pm 2, \\ Q &\approx \frac{\ln l_0 - \ln l_-}{\ln l_+ - \ln l_-}\frac{S(l_+) - S(l_0)}{\ln l_+ - \ln l_0} \\ &\quad + \frac{\ln l_+ - \ln l_0}{\ln l_+ - \ln l_-}\frac{S(l_0) - S(l_-)}{\ln l_0 - \ln l_-}, \end{aligned} \tag{11}$$

where $[L/4]$ denotes the smallest integer larger than or equal to $L/4$. The Q s for various $t_\downarrow$ and L are computed and the results are presented in figure 10 (a). For each curve, there exists a region where Q quickly drops towards zero. This is the critical region where the phase transition occurs. For better illustration, we give the first derivatives in figure 10 (b). For each line the peak locates the critical point $t_{\downarrow c}$. Then we perform scaling with $1/L$, as shown in the inset, and find that in the thermodynamic limit $t_{\downarrow c} \approx 0.32$.

The above studies show that the two-site entropy is not a sharp indicator of the phase transition of the half-filling AHM, although it shows distinct behaviors in the two phases. The block entropy, however, is useful for marking the phase transition.

4. Summary

To summarize, we have studied the ground state phase diagram of the asymmetric Hubbard chain by means of entanglement. The middle-two-site entropy S_2 and the block entropy $S(l)$ are computed for open chains using the DMRG method.

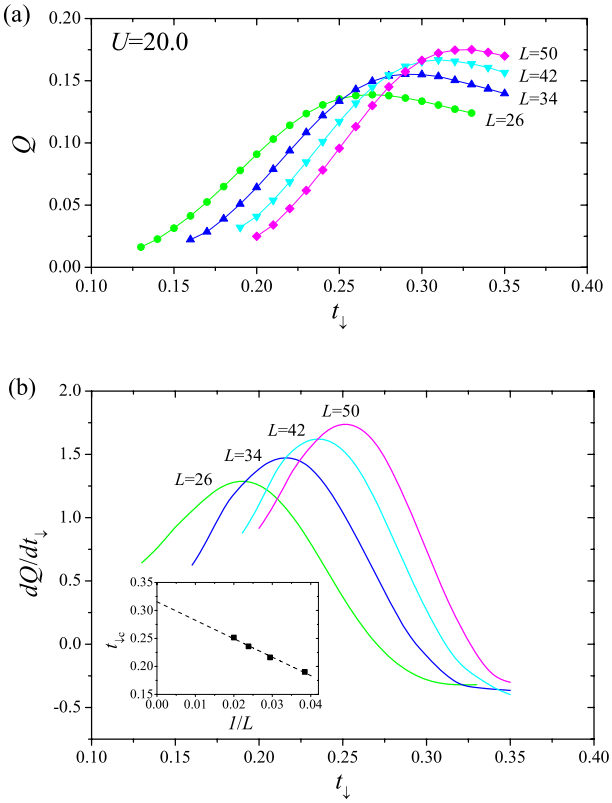

Figure 10. (a) The parameter Q, as calculated from equation (11), against $t_\downarrow$ for different chain lengths L at half-filling and fixed $U = 20.0$. (b) The first derivatives of the curves in (a). For each line the peak locates the critical point $t_{\downarrow c}$. Based on the scaling with $1/L$, the $t_{\downarrow c}$ in the thermodynamic limit can be obtained, as shown in the inset.

In the case of away from half-filling, we found that S_2 is a good indicator of phase transition between the DW phase and PS phase. The S_2 function of $t_\downarrow$ displays a sharp change at the transition point. This phase transition is deduced to be the Landau type. We performed scaling studies and presented the phase diagram. Besides, the block entropy $S(l)$ is also a good indicator of phase transition as long as l is long enough. The block entropy in the DW phase is higher than that in the PS phase.

On the other hand, in the case of half-filling, S_2 as a function of $t_\downarrow$ shows different behaviors in the Hubbard phase and FK phase. There is no sharp change of S_2 in any derivatives as the phase transition is Kosterlitz–Thouless like. Chains with different lengths were studied and we found that two families of curves are formed according to the parities of the chains due to singlet formations. Besides, the scaling behaviors of S_2 with chain length L in the two phases are different. S_2 scales as $1/\sqrt{L}$ in the Hubbard phase but scales as $\exp(-L/\xi)$ in the FK phase. The block entropy $S(l)$ also shows different behaviors in the two phases. In the Hubbard phase $S(l)$ changes algebraically, while in the FK phase it changes exponentially. By applying the concepts in conformal field theory, we propose to compute the parameter Q from the block entropies and show that Q is a valid indicator of the phase transition.

The above studies reflect certain correlations between entanglement and phase transition. They consolidate the idea that the entropy of a part of a system provides fruitful information about the whole system based on the superposition principle of quantum mechanics.

Acknowledgments

This work is supported by the Earmarked Grant for Research from the Research Grants Council of HKSAR, China (project nos 400906 and N_CUHK204/05).

References

[1] Sachdev S 2000 *Quantum Phase Transitions* (Cambridge: Cambridge University Press)
[2] Einstein A, Podolsky B and Rosen N 1935 *Phys. Rev.* **47** 777
[3] Osterloh A, Amico L, Falci G and Fazio R 2002 *Nature (London)* **416** 608
Osborne T J and Nielsen M A 2002 *Phys. Rev.* A **66** 032110
Gu S J, Lin H Q and Li Y Q 2003 *Phys. Rev.* A **68** 042330
Campos Venuti L, Degli Esposti Boschi C, Roncaglia M and Scaramucci A 2006 *Phys. Rev.* A **73** 010303(R)
Su S Q, Song J L and Gu S J 2006 *Phys. Rev.* A **74** 032308
Chen Y, Zanardi P, Wang Z D and Zhang F C 2006 *New J. Phys.* **8** 97
Cao J, Cui X, Qi Z, Lu W, Niu Q and Wang Y 2007 *Phys. Rev.* B **75** 172401
[4] Vidal G, Latorre J I, Rico E and Kitaev A 2003 *Phys. Rev. Lett.* **90** 227902
[5] Wu L-A, Sarandy M S and Lidar D A 2004 *Phys. Rev. Lett.* **93** 250404
[6] Larsson D and Johannesson H 2006 *Phys. Rev.* A **73** 042320
[7] Lin H Q, Gagliano E R, Campbell D K, Fradkin E H and Gubernatis J E 1995 *The Physics and the Mathematical Physics of the Hubbard Model* ed D Baeriswyl *et al* (New York: Plenum) pp 315–27
[8] Gu S J, Deng S S, Li Y Q and Lin H Q 2004 *Phys. Rev. Lett.* **93** 086402
Deng S S, Gu S J and Lin H Q 2006 *Phys. Rev.* B **74** 045103
[9] Anfossi A, Giorda P, Montorsi A and Traversa F 2005 *Phys. Rev. Lett.* **95** 056402
[10] Legeza Ö and Sólyom J 2006 *Phys. Rev. Lett.* **96** 116401
[11] Gu S J, Fan R and Lin H Q 2007 *Phys. Rev.* B **76** 125107
[12] Larsson D and Johannesson H 2005 *Phys. Rev. Lett.* **95** 196406
Anfossi A, Degli Esposti Boschi C, Montorsi A and Ortolani F 2006 *Phys. Rev.* B **73** 085113
Sacramento P D, Nogueira P, Vieira V R and Dugaev V K 2007 *Phys. Rev.* B **76** 184517
[13] White S R 1992 *Phys. Rev. Lett.* **69** 2863
White S R 1993 *Phys. Rev.* B **48** 10345
[14] Schollwöck U 2005 *Rev. Mod. Phys.* **77** 259
[15] Emery V J 1987 *Phys. Rev. Lett.* **58** 2794
[16] Varma C M 1985 *Comments Solid State Phys.* **11** 221
[17] Liu W V, Wilczek F and Zoller P 2004 *Phys. Rev.* A **70** 033603
[18] Cazalilla M A, Ho A F and Giamarchi T 2005 *Phys. Rev. Lett.* **95** 226402
[19] Fáth G, Domański Z and Lemański R 1995 *Phys. Rev.* B **52** 13910
[20] Ueltschi D 2004 *J. Stat. Phys.* **116** 681
[21] Macedo C A and deSouza A M C 2002 *Phys. Rev.* B **65** 153109
[22] Wang Z G, Chen Y G and Gu S J 2007 *Phys. Rev.* B **75** 165111
[23] Hubbard J 1963 *Proc. R. Soc.* A **276** 238
[24] Lieb E H and Wu F Y 1968 *Phys. Rev. Lett.* **20** 1445
[25] Essler F H L, Frahm H, Göhmann F, Klümper A and Korepin V E 2005 *The One-Dimensional Hubbard Model* (Cambridge: Cambridge University Press)
[26] Falicov L M and Kimball J C 1969 *Phys. Rev. Lett.* **22** 997
Ramirez R, Falicov L M and Kimball J C 1970 *Phys. Rev.* B **2** 3383
[27] Brandt U 1991 *J. Low Temp. Phys.* **84** 477
Freericks J K, Gruber Ch and Macris N 1999 *Phys. Rev.* B **60** 1617
[28] Lemberger P 1992 *J. Phys. A: Math. Gen.* **25** 715
[29] Kennedy T and Lieb E 1986 *Physica* A **138** 320
Lebowitz J and Macris N 1994 *Rev. Math. Phys.* **6** 927
[30] Freericks J K and Falicov L M 1990 *Phys. Rev.* B **41** 2163
Freericks J K, Lieb E H and Ueltschi D 2002 *Phys. Rev. Lett.* **88** 106401
Freericks J K and Zlatic V 2003 *Rev. Mod. Phys.* **75** 1333
[31] Lin H Q 1991 *Phys. Rev.* B **44** 7151
[32] Kennedy T and Lieb E H 1986 *Physica* A **138** 320
[33] Emery V J, Kivelson S A and Lin H Q 1990 *Phys. Rev. Lett.* **64** 475
[34] Korepin V E 2004 *Phys. Rev. Lett.* **92** 096402
[35] Calabrese P and Cardy J 2004 *J. Stat. Mech.* P06002
Calabrese P and Cardy J 2005 *J. Stat. Mech.* P04010
[36] Legeza Ö, Röder J and Hess B A 2003 *Phys. Rev.* B **67** 125114
[37] Legeza Ö and Sólyom J 2004 *Phys. Rev.* B **70** 205118
[38] White S R 1996 *Phys. Rev. Lett.* **77** 3633
[39] Yang C N and Yang C P 1966 *Phys. Rev.* **150** 321
Yang C N and Yang C P 1966 *Phys. Rev.* **150** 327
[40] Kosterlitz J M and Thouless D J 1973 *J. Phys. C: Solid State Phys.* **6** 1181